Tunable high-order photonic band gaps of ultraviolet light in cold atoms

Yan Zhang,[1,2] Yi-Mou Liu,[3] Xue-Dong Tian,[3] Tai-Yu Zheng,[1] and Jin-Hui Wu[1,2,*]

[1]*School of Physics, Northeast Normal University, Changchun 130024, People's Republic of China*

[2]*Center for Quantum Sciences, Northeast Normal University, Changchun 130117, People's Republic of China*

[3]*College of Physics, Jilin University, Changchun 130012, People's Republic of China*

(Received 10 September 2014; published 20 January 2015)

We study a five-level quasi-Λ system of cold atoms for achieving high-order photonic band gaps (PBGs) probed by an ultraviolet field in two cases where either an infrared or a visible control field works in the standing-wave configuration to induce one atomic grating. Transfer-matrix calculations for appropriate rubidium levels demonstrate that three fifth-order band gaps or two second-order band gaps can be generated near the probe resonance when the standing-wave control field is modulated to satisfy relevant Bragg conditions in the regime of electromagnetically induced transparency. These high-order PBGs, as characterized by homogeneous high reflectivities, can be dynamically tuned in positions and widths on demand and may be extended to develop efficient devices (like diodes and reflectors) for manipulating weak high-frequency light with strong low-frequency light.

DOI: 10.1103/PhysRevA.91.013826 PACS number(s): 42.50.Gy, 42.70.Qs, 32.80.Qk, 42.25.Fx

I. INTRODUCTION

The ability to manipulate photon flows in complex artificial structures or materials has attracted a lot of interest due to its potential applications in developing various smaller and faster photonic circuits and devices [1–3]. As an outstanding complex artificial structure, photonic crystals (PCs) [4,5] can mold photon flows via the widely used technique of photonic band gaps (PBGs) in which electromagnetic fields are prohibited to propagate owing to multiple Bragg reflection. Typically, first-order PBGs are exploited in real applications and relevant PCs are required to have a spatial period equivalent to the half wavelength of a controlled light signal. Then, to manipulate photon flows in the ultraviolet (UV) or even higher-frequency region, one has to be confronted with many technical difficulties, e.g., in accurately fabricating Bragg gratings of too small periods [6]. One solution is to exploit high-order PBGs with short-wavelength light signals controlled by long-period Bragg gratings, which is why in the past few years many works have focused on PCs exhibiting high-order PBGs [6–11].

On the other hand, PBGs usually cannot be changed on demand because they are determined once PCs have been grown with certain structures [5,12]. Nevertheless, the dynamic manipulation of photon flows with tunable PBGs is often desired for all-optical devices and circuits in communication networks. This nontrivial task may be attained in the regime of electromagnetically induced transparency (EIT) [13,14], e.g., when a standing-wave (SW) field is adopted in a Λ-type atomic system to induce spatially periodic quantum coherence [12]. The underlying physics is that, in an EIT window with sufficiently reduced absorption, it is viable to manipulate periodic refractive dispersion to fulfill Bragg conditions and therefore generate tunable PBGs [12,15–18]. Relevant predictions have been experimentally verified with visible PBGs manifested by reflectivity plateaus sensitive to frequencies and intensities of control fields [19–21]. However, it remains challenging to realize tunable short-wavelength PBGs, e.g., in three-level Λ-type atomic systems, due to the lack of strong coherent fields in the UV and x-ray regions, though relevant quantum coherence effects have attracted some attention [22–25].

Here we investigate the possibility of generating high-order PBGs of a UV probe field in a five-level quasi-Λ system with a visible or infrared SW control field. This quasi-Λ system interacts with the probe field in the left arm while the auxiliary, coupling, and dressing fields interact in the right arm. First we choose appropriate states of ^{87}Rb atoms to satisfy Bragg condition $5\lambda_p \simeq \lambda_s$ with the infrared dressing field set in the SW configuration. In this case, three fifth-order PBGs are found to arise at different detunings of the probe field when all other fields are near resonant with relevant transitions. These PBGs, however, correspond to slightly different SW periods as determined by a small angle between forward (FW) and backward (BW) beams of the SW dressing field. Then we choose appropriate states of ^{87}Rb atoms to satisfy Bragg condition $2\lambda_p \simeq \lambda_s$ with the visible coupling field set in the SW configuration. In this case, no second-order PBGs can be established at any detunings of the probe field when all other fields are near resonant with relevant transitions. If the auxiliary and coupling fields are far detuned instead but keep two-photon resonance, however, a doublet of second-order PBGs arises at two symmetric probe detunings as the five-level system reduces effectively into a four-level system. Such nth-order UV PBGs are characterized by experimentally accessible and dynamically tunable reflectivity plateaus near boundaries of nth Brillouin zones. We expect our numerical results to be instructive in developing quantum control techniques and efficient photonic devices in the UV and even shorter-wavelength regions for achieving all-optical light information processing and communication [26,27].

II. MODEL AND EQUATIONS

We consider a five-level quasi-Λ system of cold atoms shown in Fig. 1(a). The dipole-allowed transition from level $|1\rangle$ to level $|5\rangle$ is probed by a weak UV light field of frequency

*Corresponding author: jhwu@nenu.edu.cn

(amplitude) ω_p (E_p). Other dipole-allowed transitions $|2\rangle \leftrightarrow |3\rangle$, $|3\rangle \leftrightarrow |4\rangle$, and $|4\rangle \leftrightarrow |5\rangle$ are driven by three strong visible or infrared light fields of frequencies (amplitudes) ω_a (E_a), ω_c (E_c), and ω_d (E_d), respectively. The auxiliary field ω_a is always kept in the traveling-wave configuration while the coupling (dressing) field will be set in the SW configuration along the x direction in the first (second) case as shown below.

With the electric dipole and rotating-wave approximations, we obtain the interaction Hamiltonian

$$H_I = -\hbar \begin{bmatrix} 0 & 0 & 0 & 0 & \Omega_p^* \\ 0 & \Delta_p - \Delta_d & \Omega_a^* & 0 & 0 \\ 0 & \Omega_a & \Delta_p - \Delta_d + \Delta & \Omega_c^* & 0 \\ 0 & 0 & \Omega_c & \Delta_p - \Delta_d & \Omega_d^* \\ \Omega_p & 0 & 0 & \Omega_d & \Delta_p \end{bmatrix} \tag{1}$$

where relevant detunings are defined as $\Delta_p = \omega_p - \omega_{51}, \Delta = \omega_a - \omega_{32} = \omega_{43} - \omega_c$ (the auxiliary and coupling fields are assumed to exhibit detunings of identical magnitudes but opposite signs), and $\Delta_d = \omega_d - \omega_{54}$ while Rabi frequencies are denoted by $\Omega_p = E_p d_{15}/2\hbar, \Omega_a = E_a d_{23}/2\hbar, \Omega_c = E_c d_{34}/2\hbar$, and $\Omega_d = E_d d_{45}/2\hbar$. In addition, ω_{ij} (d_{ij}) represents the resonant frequency (dipole moment) on atomic transition $|i\rangle \leftrightarrow |j\rangle$.

Starting from Eq. (1), it is straightforward to obtain the motion equations of density-matrix elements

$$\begin{aligned} \partial_t \rho_{21} &= -\gamma'_{21}\rho_{21} + i\Omega_a^*\rho_{31}, \\ \partial_t \rho_{31} &= -\gamma'_{31}\rho_{31} + i\Omega_a\rho_{21} + i\Omega_c^*\rho_{41}, \\ \partial_t \rho_{41} &= -\gamma'_{41}\rho_{41} + i\Omega_c\rho_{31} + i\Omega_d^*\rho_{51}, \\ \partial_t \rho_{51} &= -\gamma'_{51}\rho_{51} + i\Omega_d\rho_{41} + i\Omega_p \end{aligned} \tag{2}$$

valid in the weak probe limit. Equations (2) are constrained by $\sum \rho_{ii} = 1$ and $\rho_{ij} = \rho_{ji}^*$ together with the assumption $\rho_{11} = 1, \rho_{22} = \rho_{33} = \rho_{44} = \rho_{55} = 0$, and $\rho_{23} = \rho_{24} = \rho_{25} = \rho_{34} = \rho_{35} = \rho_{45} = 0$. We have also set $\gamma'_{21} = \gamma_{21} + i(\Delta_d - \Delta_p), \gamma'_{31} = \gamma_{31} + i(\Delta_d - \Delta_p - \Delta), \gamma'_{41} = \gamma_{41} + i(\Delta_d - \Delta_p)$, and $\gamma'_{51} = \gamma_{51} - i\Delta_p$ as the complex dephasing rates of relevant density-matrix elements with γ_{ij} being the real counterparts of complex γ'_{ij}.

Setting $\partial_t \rho_{ij} = 0$ to solve Eq. (2) in the steady state, we can obtain the complex probe susceptibility

$$\chi_{p5} = \frac{N_0|d_{15}|^2}{2\varepsilon_0\hbar} \times \frac{\rho_{51}}{\Omega_p} = i\frac{N_0|d_{15}|^2}{2\varepsilon_0\hbar} \times \frac{\gamma'_{41}\gamma'_{31}\gamma'_{21} + \gamma'_{41}\Omega_a^2 + \gamma'_{21}\Omega_c^2}{\gamma'_{51}\gamma'_{41}\gamma'_{31}\gamma'_{21} + \gamma'_{51}\gamma'_{41}\Omega_a^2 + \gamma'_{51}\gamma'_{21}\Omega_c^2 + (\gamma'_{31}\gamma'_{21} + \Omega_a^2)\Omega_d^2} \tag{3}$$

where N_0 is the volume density of a homogeneous sample of cold atoms. With Eq. (3) it is easy to examine the complex refractive index $n_{p5} = \sqrt{1 + \chi_{p5}}$ whose imaginary and real parts govern, respectively, local absorptive and dispersive properties of a weak probe field.

When the coupling (case 1) or dressing (case 2) field is set to work in the SW configuration, we should describe it by a spatially modulated Rabi frequency

$$\Omega_s(x) = \Omega_{s+}e^{+ik_s x} + \Omega_{s-}e^{-ik_s x} \tag{4}$$

with the period $a_s = \lambda_s/(2\cos\theta_s)$ along the x direction. Here $2\theta_s$ is a small angle between the FW (Ω_{s+}) and BW (Ω_{s-}) components of a spatially modulated coupling (case 1) or dressing (case 2) field. Then refractive index n_{p5} is also periodically modulated so that the atomic sample is driven into a one-dimensional atomic grating and multiple Bragg scattering yields complicated optical responses inaccessible directly through Eq. (3).

In what follows we adopt the transfer-matrix method to examine whether high-order PBGs open up for a UV probe field in the presence of an infrared or visible SW field. To this end, we first evaluate a 2×2 unimodular transfer matrix M_j as in Refs. [28,29], which describes the propagation of a weak probe field through the jth SW period and is restricted by the Bloch condition, starting with the probe susceptibility χ_{p5}

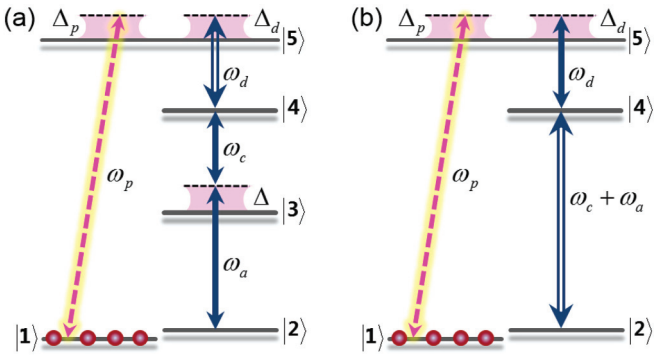

FIG. 1. (Color online) (a) Schematic diagram of a five-level quasi-Λ system of cold atoms driven into the EIT regime by a weak probe field ω_p, a strong auxiliary field ω_a, a strong-coupling field ω_c, and a strong dressing field ω_d. (b) Schematic diagram of a four-level quasi-Λ system with two far-detuned single-photon transitions $|2\rangle \overset{\omega_a}{\longleftrightarrow} |3\rangle$ and $|3\rangle \overset{\omega_c}{\longleftrightarrow} |4\rangle$ replaced by one resonant two-photon transition $|2\rangle \overset{\omega_a+\omega_c}{\longleftrightarrow} |4\rangle$. An infrared dressing field ω_d in (a) and a visible coupling field ω_c in (b) are set in the SW configuration to attain fifth-order and second-order PBGs for a UV probe field, respectively.

in Eq. (3):

$$\begin{bmatrix} E_p^+(x+a_s) \\ E_p^-(x+a_s) \end{bmatrix} = M_j(\Delta_p) \begin{bmatrix} E_p^+(x) \\ E_p^-(x) \end{bmatrix} = \begin{bmatrix} e^{i\kappa a_s} E_p^+(x) \\ e^{i\kappa a_s} E_p^-(x) \end{bmatrix} \quad (5)$$

where E_p^+ and E_p^- denote the FW and BW probe electric fields, respectively. Equation (5) allows one to check the expected high-order PBGs via the complex Bloch wave vector $\kappa = \kappa' + i\kappa''$ with the requirement

$$\cos(\kappa a_s) = Tr[M_j(\Delta_p)]/2. \quad (6)$$

Note, in particular, that boundaries of the nth Brillouin zone are reached when we have $\kappa' = \pm n\pi/a_s$ with $n = 1,2,3,\ldots,$ indicating $Tr[M_j(\Delta_p)] = \pm 2$.

It is well known that a FW incident probe field will experience multiple Bragg scattering to generate considerable BW photons when it propagates through a multilayer periodic structure, and PBGs are expected to open up at boundaries of the nth Brillouin zone if the Bragg condition $n\lambda_p \simeq \lambda_s$ (i.e., $\omega_p \simeq n\omega_s$) is satisfied. That is, we will obtain nth-order PBGs near the probe resonance where $\kappa' \simeq \pm n\pi/a_s$ and $\kappa'' \neq 0$. The existence of nth-order PBGs can be further verified by examining probe reflectivity and probe transmissivity:

$$R(\Delta_p) = \left| \frac{M_{(12)}(\Delta_p)}{M_{(22)}(\Delta_p)} \right|^2, \qquad T(\Delta_p) = \left| \frac{1}{M_{(22)}(\Delta_p)} \right|^2 \quad (7)$$

directly accessible in experiment, contrary to κ' and κ'' of the Bloch wave vector. Here $M_{(ij)}$ is one matrix element of $M = M_1 \cdots M_j \cdots M_N$, the total transfer matrix of an atomic sample with N SW periods.

III. RESULTS AND DISCUSSION

In this section, we examine via numerical calculations the efficient generation of high-order PBGs in two cases where either a coupling (ω_c) or dressing (ω_d) field is set in the SW configuration. One difficulty of generating high-order PBGs via spatially modulated atomic coherence lies in the fact that we have to find appropriate atomic levels with relevant resonant frequencies approximately satisfying the Bragg condition $\lambda_p \simeq n\lambda_s$. In addition, it is usually difficult to obtain high reflectivities and large bandwidths for high-order PBGs because the Bragg condition $\lambda_p \simeq n\lambda_s$ is more fragile to parameter fluctuations as the order n is increased. Therefore it is essential to accurately control the SW coupling or dressing field in terms of frequency ω_s, amplitude E_s, and angle θ_s to maximize the stability of high-order PBGs.

A. Fifth-order UV PBGs

We first consider the case in which levels $|1\rangle$, $|2\rangle$, $|3\rangle$, $|4\rangle$, and $|5\rangle$ correspond, respectively, to $|F = 2, m_F = 2\rangle$ of $5S_{1/2}$, $|F = 1, m_F = 0\rangle$ of $5S_{1/2}$, $|F = 2, m_F = 1\rangle$ of $5P_{1/2}$, $|m_J + m_I = 2\rangle$ of $7S_{1/2}$, and $|m_J + m_I = 3\rangle$ of $15P_{3/2}$ for cold ^{87}Rb atoms in the presence of a moderate magnetic field [30–32]. In this case, all the applied fields should have an exact σ^+ polarization and we can choose the dressing field

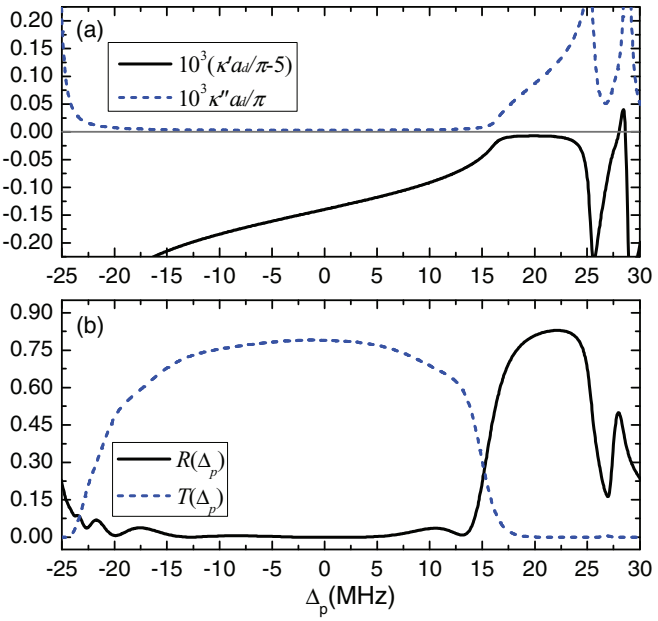

FIG. 2. (Color online) (a) Real (black solid) and imaginary (blue dashed) parts of the Bloch wave vector. (b) Reflectivity (black solid) and transmissivity (blue dashed) vs probe detuning Δ_p with $\Omega_{d+} =$ 168 MHz, $\Omega_{d-} = 143$ MHz, $\Omega_c = 4.0$ MHz, $\Omega_a = 60$ MHz, $\Delta_d = \Delta = 0, \gamma_{21} = 0.2$ kHz, $\gamma_{31} = 5.8$ MHz, $\gamma_{41} = 0.6$ MHz, $\gamma_{51} = 0.2$ MHz, $\theta_d = 7.78^\circ$, $d_{15} = 1.6 \times 10^{-30}$ C m, $N_0 = 8.0 \times 10^{12}$ cm^{-3}, and $L = 9.8$ mm. Relevant field wavelengths are $\lambda_p = 303$ nm, $\lambda_d =$ 1501 nm, $\lambda_c = 728$ nm, and $\lambda_a = 795$ nm [30–32].

of wavelength $\lambda_d \simeq 1501$ nm (infrared) to work in the SW configuration. Thus it is possible to attain a SW grating of period $a_d \simeq 757.5$ nm by setting $\theta_d \simeq 7.78^\circ$ so that a probe field of wavelength $\lambda_p \simeq 303$ nm (UV) may experience the fifth-order PBGs with $5\lambda_p \simeq 2a_d$. In principle, three such PBGs will arise at different probe detunings, each close to the center of a spatially modulated EIT window. Note that a quasi-Λ system can be attained without involving other Zeeman or Paschen-Back levels [33] even if the FW and BW dressing beams have also the π and σ^- polarizations because $m_J + m_I$ cannot equal to 3 or 4 for $7S_{1/2}$ [34].

With Eqs. (3)–(7), we can plot in Fig. 2 real and imaginary parts of the Bloch wave vector (a) as well as reflectivity and transmissivity of the probe intensity (b) versus probe detuning Δ_p to examine first the central PBG near probe resonance. Figure 2(a) clearly shows that, in the region of $\Delta_p \in \{18,25\}$ MHz, a stop band opens up near one boundary of the fifth Brillouin zone as manifested in $\kappa' a_d \simeq 5\pi$ and $\kappa'' a_d \neq 0$. The existence of this fifth-order PBG is further verified by a plateau of high reflectivity (~82%) and a basin of low transmissivity (~0.1%) in Fig. 2(b). In the region of $\Delta_p \in \{-12,7\}$ MHz, however, we have instead $\kappa' a_d \neq 5\pi$ and $\kappa'' a_d \simeq 0$ so that it is viable to get a nearby allowed band of high transmissivity (~78%) and low reflectivity (~0.1%). Positions of the stop and allowed bands may be reversed with respect to probe resonance $\Delta_p = 0$ by modulating angle θ_d of the FW and BW dressing field beams [12].

In Fig. 3 we plot probe reflectivity R and transmissivity T versus probe detuning Δ_p in a much wider region to check whether we can simultaneously get all three expected

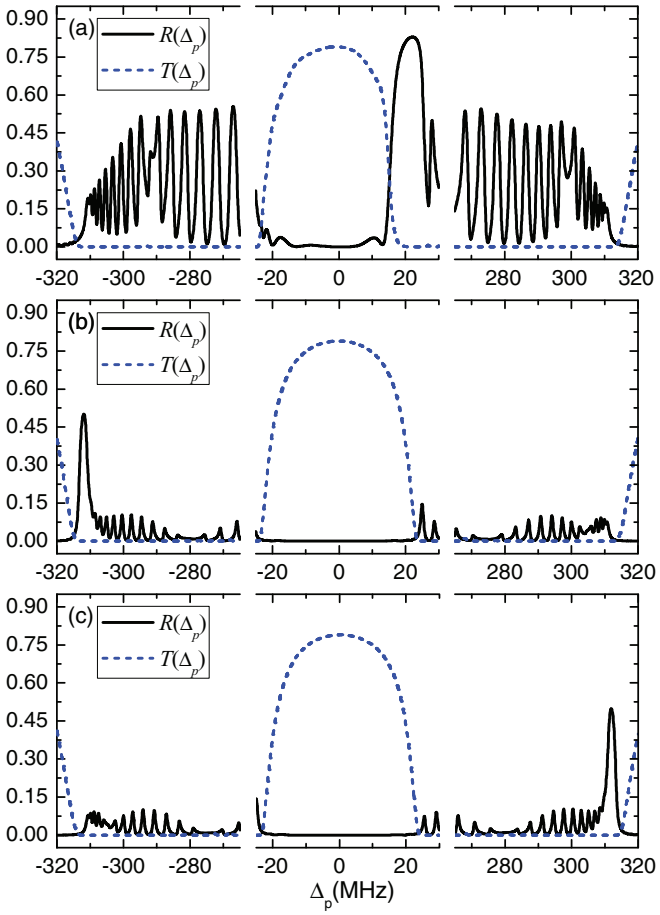

FIG. 3. (Color online) Probe reflectivity (black solid) and transmissivity (blue dashed) vs probe detuning Δ_p with $\theta_d = 7.78^\circ$ (a), $\theta_d = 7.70^\circ$ (b), and $\theta_d = 7.89^\circ$ (c). Other parameters are the same as in Fig. 2.

fifth-order PBGs. Figure 3(a) clearly shows that the two side PBGs are not well established (like the central one) in the presence of many reflective interference fringes with the same parameters as in Fig. 2. Slightly modifying angle θ_d (period a_d), however, we can observe a well-developed side PBG around $\Delta_p = -312$ MHz [Fig. 3(a)] or $\Delta_p = +312$ MHz [Fig. 3(c)] at the expense of destroying the central PBG. The results in Fig. 3 indicate that the best development of various PBGs requires slightly different parameters (angle θ_d and period a_d) due to the fragility of high-order Bragg conditions. In addition, the central PBG is easier to develop into a wider and higher plateau of reflectivity as compared to the side PBGs; a nearby allowed band of high transmissivity is seen to become wider as one stop band of high reflectivity degrades into low residual fringes.

B. Second-order UV PBGs

We then consider the case in which levels $|1\rangle$, $|2\rangle$, $|3\rangle$, $|4\rangle$, and $|5\rangle$ correspond, respectively, to $|F = 2, m_F = 1\rangle$ of $5S_{1/2}$, $|F = 1, m_F = 1\rangle$ of $5S_{1/2}$, $|F = 2, m_F = 2\rangle$ of $5P_{1/2}$, $|m_J + m_I = 3\rangle$ of $6D_{3/2}$, and $|m_J + m_I = 2\rangle$ of $11P_{3/2}$ for cold ^{87}Rb atoms in the presence of a moderate magnetic field [30–32]. In this case, the dressing field and other three fields are required to have, respectively, an exact σ^- polarization and an exact σ^+ polarization. Here we choose the coupling field of wavelength $\lambda_c \simeq 621$ nm (visible) to work in the SW configuration. Thus it is possible to attain a SW grating of period $a_c \simeq 311$ nm by setting $\theta_c \simeq 3.25^\circ$ such that a probe field of wavelength $\lambda_p \simeq 311$ nm (UV) may experience the second-order PBGs with $2\lambda_p \simeq 2a_c$. Once again, three PBGs are expected to arise at different probe detunings and an ideal quasi-Λ system can be attained even if the FW and BW coupling beams have the π and σ^- polarizations.

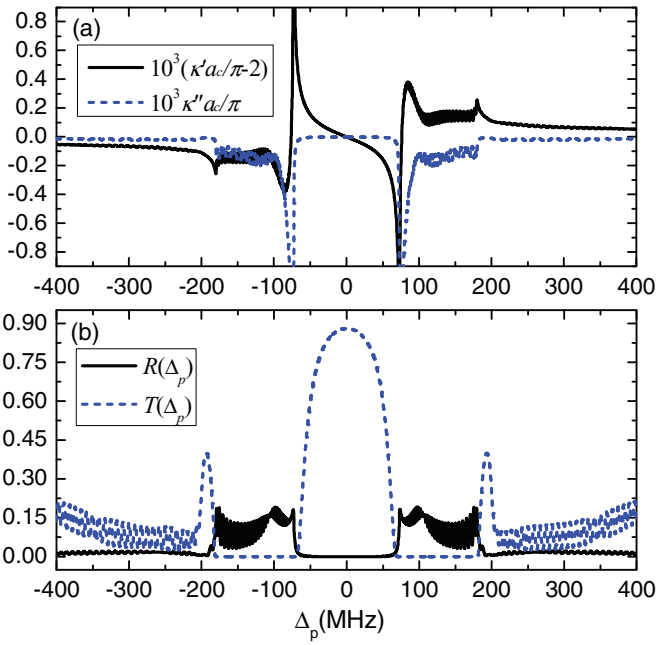

FIG. 4. (Color online) (a) Real (black solid) and imaginary (blue dashed) parts of the Bloch wave vector. (b) Reflectivity (black solid) and transmissivity (blue dashed) vs probe detuning Δ_p with $\Omega_{c+} = \Omega_{c-} = 210$ MHz, $\Omega_d = 180$ MHz, $\Omega_a = 200$ MHz, $\Delta_d = \Delta = 0, \gamma_{21} = 0.2$ kHz, $\gamma_{31} = 5.8$ MHz, $\gamma_{41} = 1.8$ MHz, $\gamma_{51} = 0.28$ MHz, $\theta_c = 3.25^\circ$, $d_{15} = 2.0 \times 10^{-30}$ C m, $N_0 = 5.0 \times 10^{12}$ cm^{-3}, and $L = 6.8$ mm. Relevant field wavelengths are $\lambda_p = 311$ nm, $\lambda_d = 2910$ nm, $\lambda_c = 621$ nm, and $\lambda_a = 795$ nm [30–32].

However, numerical results in Fig. 4 show that it is not possible to attain well-developed PBGs when the auxiliary (ω_a), coupling (ω_c), and dressing (ω_d) fields are resonant with relevant transitions. The underlying physics can be inferred from Eq. (3) where the coefficients of Ω_c^2 are much smaller than those of Ω_a^2 and Ω_d^2 because γ_{21} is a small quantity as compared to other dephasing rates and all Rabi frequencies. To have well-developed PBGs, we should choose appropriate parameters to amplify the periodic modulation of a SW coupling field on the probe susceptibility. This is done by setting the auxiliary and coupling fields to be far detuned from relevant transitions with a sufficiently large $|\Delta|$ [35,36]. Then we may safely reduce the five-level quasi-Λ system [Fig. 1(a)] into a four-level quasi-Λ system [Fig. 1(b)] with the probe susceptibility becoming instead

$$\chi_{p4} = i\frac{N_0|d_{15}|^2}{2\varepsilon_0\hbar}\frac{\gamma'_{41}\gamma'_{21} + \Omega_e^2}{\gamma'_{51}\gamma'_{41}\gamma'_{21} + \gamma'_{51}\Omega_e^2 + \gamma'_{21}\Omega_d^2} \tag{8}$$

where $\Omega_e = \Omega_a\Omega_c/\Delta$ is the effective Rabi frequency on the two-photon transition $|2\rangle \overset{\omega_c+\omega_s}{\longleftrightarrow} |4\rangle$.

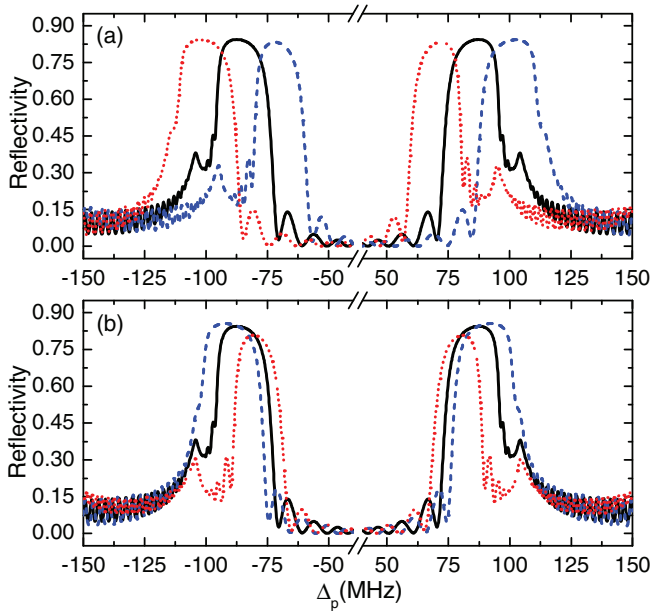

FIG. 5. (Color online) Probe reflectivity vs probe detuning Δ_p with $\Omega_{e+} = \Omega_{e-} = 80$ MHz, $\Delta_d = 0$ (black solid); 20 MHz (blue dashed); and -20 MHz (red dotted) in panel (a) and $\Delta_d = 0, \Omega_{e+} = \Omega_{e-} = 80$ MHz (black solid), 90 MHz (blue dashed), and 70 MHz (red dotted) in panel (b). Other parameters are the same as in Fig. 4 except $\Omega_d = 104$ MHz.

By replacing Eq. (3) with Eq. (8), we plot in Fig. 5 probe reflectivity R versus probe detuning Δ_p to examine the potential second-order PBGs. We find that a doublet of second-order PBGs arises near one boundary of the second Brillouin zone as manifested by two symmetric plateaus of high reflectivity ($\sim$85%). We would like to stress that this pair of second-order PBGs is generated within a double EIT structure [29,37–39] while first-order double PBGs have been predicted in a four-level N system [40]. In addition, it is clear that these second-order PBGs (likewise for those fifth-order PBGs) can be dynamically tuned in positions and widths by modulating the SW coupling field. Finally we have applied a perfect SW coupling field ($\Omega_{e+} = \Omega_{e-}$) to induce second-order PBGs because the required EIT background survives even at the SW nodes due to $\Omega_d \neq 0$ [see Fig. 1(a)]. In contrast, an imperfect SW dressing field ($\Omega_{d+} \neq \Omega_{d-}$) has to be used to induce fifth-order PBGs, otherwise the required EIT background cannot be guaranteed at the SW nodes [see Fig. 1(b)]. Both second-order and fifth-order PBGs will be blurred if significant absorption exists at the SW nodes in the absence of an EIT background [12].

It is worth stressing that resonant dipole-dipole interactions should be considered even for low-lying excited states when average atomic separations are smaller than relevant transition wavelengths [41,42], but in the weak probe limit most atoms are populated at the ground level $|1\rangle$ so that it is enough to consider only resonant dipole-dipole interactions on the most important $|1\rangle \leftrightarrow |5\rangle$ transition. That is why we can neglect resonant dipole-dipole interactions when the probe wavelength 303 (311) nm in the first (second) case is clearly larger than the atomic separation for $N_0 = 8.0 \times 10^{12}$ cm^{-3} (5.0×10^{12} cm^{-3}). In addition, the hyperfine levels of $6D_{3/2}, 7S_{1/2}, 11P_{3/2}$, and $15P_{3/2}$ have very small energetic separations, which then requires us to carefully treat the nonresonant scattering. The fact is, however, that nonresonant scattering can be safely neglected when a moderate magnetic field is applied to lift the degeneracy of all Zeeman and Paschen-Back levels in the weak probe limit.

IV. CONCLUSIONS

In summary, we have studied a five-level quasi-Λ system of cold atoms with the goal to generate tunable high-order PBGs so that the propagation behaviors of a weak high-frequency probe field are dynamically controlled by a strong low-frequency SW field. In this quasi-Λ system, the probe field applied to drive the only left-arm transition exhibits a frequency being about the frequency sum of auxiliary, coupling, and dressing fields applied to drive the three right-arm transitions. We consider, in particular, two cases where the five levels correspond to different hyperfine states of cold ^{87}Rb atoms with the dressing (case 1) or coupling (case 2) field set in the SW configuration. In the first case, the infrared dressing field can induce three fifth-order PBGs for the UV probe field near one boundary of the fifth Brillouin zone. These fifth-order PBGs, however, correspond to slightly different periods of the SW grating and are somewhat fragile to the angle between FW and BW beams of the dressing field. In the second case, the visible coupling field can induce two second-order PBGs for the UV probe field near one boundary of the second Brillouin zone. These second-order PBGs can only be attained when the five-level system reduces into a four-level system with far-detuned auxiliary and coupling fields. Both second-order and fifth-order PBGs are manifested by characteristic spectra of the Bloch wave vector and probe reflectivity and can be dynamically tuned in positions and widths by manipulating the SW control field.

ACKNOWLEDGMENTS

This work is supported by the National Basic Research Program of China (Grant No. 2011CB921603), the National Natural Science Foundation of China (Grants No. 11174110, No. 11175044, No. 11247005, and No. 61378094), the Fundamental Research Funds for Central Universities of China (Grant No. 12QNJJ006), and the Postdoctoral Scientific Research Program of Jilin Province (Grant No. RB201330).

[1] C. M. Soukoulis, *Photonic Crystals and Light Localization in the 21st Century* (Kluwer, Dordrecht, 2001).

[2] T.-N. Oder, J. Shakya, J.-Y. Lin, and H.-X. Jiang, Appl. Phys. Lett. **83**, 1231 (2003).

[3] X. Wu, A. Yamilov, X. Liu, S. Li, V. P. Dravid, R. P. H. Chang, and H. Cao, Appl. Phys. Lett. **85**, 3657 (2004).

[4] S. John, Phys. Rev. Lett. **58**, 2486 (1987).

[5] K. Sakoda, *Optical Properties of Photonic Crystals* (Springer, Berlin, 2001).

[6] D.-W. Wang, S.-Y. Zhu, J. Evers, and M. O. Scully, arXiv:1305.3636v2.

[7] M. Straub, M. Ventura, and M. Gu, Phys. Rev. Lett. **91**, 043901 (2003).

[8] M. Scharrer, A. Yamilov, X. Wu, H. Cao, and R. P. H. Chang, Appl. Phys. Lett. **88**, 201103 (2006).

[9] S. Zarei and M. Shahabadi, J. Opt. A **10**, 085203 (2008).

[10] S. Savo, E. D. Gennaro, and A. Andreone, Opt. Express **17**, 19848 (2009).

[11] X.-D. Lu, F. Chi, T. Zhou, and S.-X. Lun, Opt. Commun. **285**, 1885 (2012).

[12] M. Artoni and G. C. La Rocca, Phys. Rev. Lett. **96**, 073905 (2006).

[13] S. E. Harris, Phys. Today **50**(7), 36 (1997).

[14] M. Fleischhauer, A. Imamoglu, and J. P. Marangos, Rev. Mod. Phys. **77**, 633 (2005).

[15] A. Andre and M. D. Lukin, Phys. Rev. Lett. **89**, 143602 (2002).

[16] X.-M. Su and B. S. Ham, Phys. Rev. A **71**, 013821 (2005).

[17] S.-Q. Kuang, R.-G. Wan, P. Du, Y. Jiang, and J.-Y. Gao, Opt. Express **16**, 15455 (2008).

[18] Y. Zhang, Y. Xue, G. Wang, C.-L. Cui, R.-G. Wang, and J.-H. Wu, Opt. Express **19**, 2111 (2011).

[19] J.-X. Zhang, H.-T. Zhou, D.-W. Wang, and S.-Y. Zhu, Phys. Rev. A **83**, 053841 (2011).

[20] H.-T. Zhou, D.-W. Wang, D. Wang, J.-X. Zhang, and S.-Y. Zhu, Phys. Rev. A **84**, 053835 (2011).

[21] A. Schilke, C. Zimmermann, and W. Guerin, Phys. Rev. A **86**, 023809 (2012).

[22] P. Ranitovic, X. M. Tong, C. W. Hogle, X. Zhou, Y. Liu, N. Toshima, M. M. Murnane, and H. C. Kapteyn, Phys. Rev. Lett. **106**, 193008 (2011).

[23] B. W. Adams, C. Buth, S. M. Cavaletto, J. Evers, Z. Harman, C. H. Keitel, A. Pálffy, A. Picón, R. Röhlsberger, Y. Rostovtsev, and K. Tamasaku, J. Mod. Opt. **60**, 2 (2013).

[24] R. Rohlsberger, T. Klein, K. Schlage, O. Leupold, and R. Ruffer, Phys. Rev. B **69**, 235412 (2004).

[25] T. E. Glover, M. P. Hertlein, S. H. Southworth, T. K. Allison, J. van Tilborg, E. P. Kanter, B. Kräsig, H. R. Varma, B. Rude, R. Santra, A. Belkacem, and L. Young, Nat. Phys. **6**, 69 (2010).

[26] D.-W. Wang, H.-T. Zhou, M.-J. Guo, J.-X. Zhang, J. Evers, and S.-Y. Zhu, Phys. Rev. Lett. **110**, 093901 (2013).

[27] S. A. R. Horsley, J.-H. Wu, M. Artoni, and G. C. La Rocca, Phys. Rev. Lett. **110**, 223602 (2013).

[28] M. Artoni, G. C. La Rocca, and F. Bassani, Phys. Rev. E **72**, 046604 (2005).

[29] Y. Zhang, J.-W. Gao, C.-L. Cui, Y. Jiang, and J.-H. Wu, Phys. Lett. A **374**, 1088 (2010).

[30] Y. Ralchenko, F.-C. Jou, D. E. Kelleher, A. E. Kramida, A. Musgrove, J. Reader, W. L. Wiese, and K. Olsen, NIST Atomic Spectra Database, http://physics.nist.gov/asd3

[31] M. S. Safronova and U. I. Safronova, Phys. Rev. A **83**, 052508 (2011).

[32] H.-R. Noh and H. S. Moon, Phys. Rev. A **85**, 033817 (2012).

[33] D. A. Steck, Rubidium 87 D line data, http://steck.us/alkalidata

[34] The probe, coupling, and auxiliary fields having an exact σ^+ polarization also will not interact with other Zeeman and Paschen-Back levels outside of this quasi-Λ system owing to the transition selection rules.

[35] D. Yan, J.-W. Gao, Q.-Q. Bao, H. Yang, H. Wang, and J.-H. Wu, Phys. Rev. A **83**, 033830 (2011).

[36] H. Wang, Y.-M. Liu, J.-W. Gao, D. Yan, R. Wang, and J.-H. Wu, Opt. Comm. **285**, 3498 (2012).

[37] Z.-G. Chang, Y.-H. Qi, Y.-P. Niu, J.-T. Zhang, and S.-Q. Gong, J. Phys. B **45**, 235401 (2012).

[38] Z.-Y. Bai, C. Hang, and G.-X. Huang, Opt. Express **21**, 17736 (2013).

[39] H. M. M. Alotaibi and B. C. Sanders, Phys. Rev. A **89**, 021802(R) (2014).

[40] R.-G. Wan, J. Kou, L. Jiang, S.-Q. Kuang, Y. Jiang, and J.-Y. Gao, Opt. Commun. **284**, 1569 (2011).

[41] S. Balik, A. L. Win, M. D. Havey, I. M. Sokolov, and D. V. Kupriyanov, Phys. Rev. A **87**, 053817 (2013).

[42] J. Pellegrino, R. Bourgain, S. Jennewein, Y. R. P. Sortais, A. Browaeys, S. D. Jenkins, and J. Ruostekoski, Phys. Rev. Lett. **113**, 133602 (2014).